Kinetics and Catalysis, Vol. 41, No. 2, 2000, pp. 211–215. Translated from Kinetika i Kataliz, Vol. 41, No. 2, 2000, pp. 233–238.

The Effect of Doping of the Ultradispersed Nickel Powder by Pyrocarbon on Oxygen Adsorption and O_{ads} + CO Reaction

I. I. Mikhalenko, A. M. Katre, and V. D. Yagodovskii

Russian University of Peoples' Friendship, Moscow, 117198 Russia

Received April 17, 1998

Abstract—Oxygen adsorption and chemisorption and the kinetics of interaction between adsorbed oxygen and CO on nickel ultradispersed powder (average size of particles, 20 nm) are studied. The ultradispersed nickel powder was dosed by the products of pyrolysis of chemisorbed ethylene (pyrocarbon) in the amount of 0.1–1.6 of a monolayer. The spectra of ferromagnetic resonance of the ultradispersed nickel powder before and after ethylene adsorption and pyrolysis and after adsorption and chemisorption of oxygen and its reduction by hydrogen are recorded. The magnetization of ultradispersed nickel powder increases upon dosing the surface with ethylene (C_2H_{4ads}) and pyrocarbon in the amount of 0.5 of a monolayer. Pyrocarbon inhibits the O_{ads} + CO reaction. The reaction orders with respect to O_{ads} and CO and the experimental activation energy change. The effects of small (less than a monolayer) and large (more than a monolayer) amounts of the modifying agent are different.

INTRODUCTION

Ultradispersed powders (UDP) of metals are of interest as objects for the studies of adsorption and catalysis because they exhibit different properties from those of bulk and supported catalysts. The characteristics of UDP depend substantially on preparation that affects the dispersion, phase composition, and the presence of admixtures, as well as the presence of other modifying agents on the surface.

UDP of nickel are active in the liquid-phase hydrogenation and dehydrogenation of hydrocarbons [1, 2] and CO hydrogenation [3]. According to the data of [3], the activity of nickel UDP prepared by electric explosion depends on the particle size. Thus, the reaction products contained methane (up to 30%), ethane, propane, ethylene, and propene if the particles of a sample have an average size of 20 nm, whereas methane was the main product (80–90%) when the particle size increased to 60 nm. UDP can be used for the preparation of supported catalysts; such UDP based on the iron-group metals are the efficient catalysts for the neutralization of exhaust gases from car engines [4, 5].

During catalytic reactions, the strong adsorption of hydrocarbons, for example, olefins leads to changes the state of the surface. Activity may either decrease (catalyst deactivation) or increase (promotion). The influence of chemisorbed reactants or special additives on the catalytic and magnetic properties of nickel UDP has not been studied yet.

The goal of this work is to study the effect of chemisorbed ethylene (pyrocarbon) on oxygen adsorption and the kinetics of interaction between O_{ads} and CO over the ultradispersed nickel powder.

EXPERIMENTAL

Characterization of samples. Nickel UDP was prepared by the electric explosion of an Ni wire containing less than 0.1% of admixtures (Cr, Cu, Fe, Zn, Mo, and W) in an argon atmosphere. The specific surface area estimated from the low-temperature nitrogen adsorption by the BET method was 33 m^2/g. The size distribution of the particles and their average diameter were determined by photon correlation spectroscopy (PCS). PCS is based on the measurement of the time dependence of the fluctuation of scattered light caused by changes in the arrangement of diffusing particles [6]. The size distribution of particles and the average size of UDP particles were determined on a computerized analyzer COULTER N4SD by measuring the diffusion coefficient of particles, which participated in the Brownian motion in a suspension. A suspension was prepared by dispersing powder by ultrasound in an organic solvent. An error in estimating the average size of particles by PCS was at most 3%. The particle sizes were 10–15 nm (11% of particles), 15–22 nm (87%), and 22–32 nm (2%); the average diameter was 20 nm. The specific surface area calculated from these data was 34 m^2/g, in good agreement with the adsorption measurements. According to X-ray phase analysis, initial UDP contained only metallic nickel. Examination of the subsurface layer by XPS (a XSAM-800 spectrometer) showed the presence mainly of nickel oxide and ~20% of metal.

Before a run, ultradispersed powder was reduced in hydrogen at 643 K. UDP surface was modified by ethylene adsorption at 298 K. Then, the samples were allowed to stay at 643 K for 0.5 h and evacuated at 623 K. The surface coverage expressed in fractions of a monolayer (ML) (θ_m) was calculated for the 1 atom C : 1 sur-

0023-1584/00/4102-0211$25.00

Table 1. Effect of ethylene adsorption and the products of its pyrolysis on the relative intensity (I_{rel}) of Ni UDP

State of sample	I_{rel} at the surface coverage θ_m by ethylene					
	0	0.1	0.2	0.3	0.4	1.6
Adsorption of C_2H_4 at 298 K	48	49	65	72	78	86
After pyrolysis (without evacuation)	47	55	69	96	71	82
After pyrolysis (with evacuation)	49	66	67	82	70	74

face atom Ni stoichiometry. That is, we assumed that one C_2H_4 molecule is adsorbed on two nickel sites (atoms). The products of ethylene pyrolysis (pyrocarbon) are CH_x species, $x = 0$ or 1 at low θ_m values ($\theta_m <$ 0.2 ML) and $x = 2$ at $\theta_m > 0.2$ ML; this was found from the amount of H_2 evolved during ethylene pyrolysis.

Magnetization was studied in an oil-free vacuum (the system was evacuated by a zeolite pump to a residual pressure of 0.013 Pa). The ferromagnetic resonance (FR) spectra were recorded at room temperature using DPPH (diphenylpicrilhydrazyl) as a standard. The FR spectra were also recorded for the island Ni film deposited in a vacuum on the quartz surface; the film had the same average size of particles as UDP. The absorption maxima in the FR spectra of the film and UDP coincided ($H_e \sim 2100$ Oe), but the FR signal for UDP was asymmetric.

For each state of the UDP sample, 7–8 spectra were recorded together with the spectra for the standard from which the integral intensities I_{Ni} and I_{st} were determined; the root-mean-square error was at most 3% for UDP and 1% for the standard. The relative integral intensities $I_{rel} = I_{Ni}/I_{st}$ were calculated with a root-mean-square error of at most 5%. The confidence intervals of I_{rel} were found with the aid of t-criterion; the two-sided confidence interval was shorter than 15–17% of the average value for the significance level of 95%. A comparison of the confidence regions of $I_{rel} \pm 3$ showed the significance of differences in the I_{rel} values, for example, 48 and 65 (Table 1). The results of measurements were processed according to [7]. FR spectra for nonmodified initial and oxygen-dosed UDP had a nearly Gaussian shape; after doping, the line was of the mixed Lorentz–Gaussian type.

The oxygen adsorption was carried out at 298 K up to 0.5 ML, and then the temperature of the sample was increased. After oxygen chemisorption, the sample was recovered by reduction in H_2 at $P_{H_2} \sim 13$ Pa and $T =$ 643 K for 0.5 h.

The kinetics of the $O_{ads} + CO \longrightarrow CO_2$ reaction was studied at 400–550 K under static conditions with CO_2 removal by freezing out. Special tests revealed that CO_2 was not formed during the contact of CO with the UDP surface containing no O_{ads}. The initial content of O_{ads} was 0.5 ML, and the initial pressure of CO P^0_{CO} was 2 Pa. The reaction orders were determined by the variation of the initial content of one of the reactants. The order with respect to O_{ads} was estimated for initial coverages (θ_0) of 0.15–0.8 ML at $P^0_{CO} = 2$ Pa. The order with respect to CO was estimated at $P^0_{CO} = 0.4$–2 Pa and $\theta_0 = 0.5$ ML. The reaction duration was 20 min in each run. The amount of UDP in the reactor was 50 mg. The volume of the reaction zone was 5 cm^3.

After catalytic runs, the X-ray phase analysis of UDP was carried out. The oxide phases were found in all the samples together with the metal phase. A substantial change in the phase composition of nonmodified and modified samples was not observed.

RESULTS AND DISCUSSION

FR spectra. A change in the shape of FR spectra for UDP after dosing by pyrocarbon indicates a weakening in the spin interaction between the nickel particles.

The 25–50 nm nickel particles are one-domain particles. Strong interaction between the resulting spins of the particles determines the Gaussian line shape. The interaction between spins in the nickel particles modified by pyrocarbon and containing chemisorbed oxygen becomes weaker; therefore, the line becomes of a mixed Gaussian–Lorentz type.

Tables 1 and 2 present the data on the magnetization of nickel UDP after various treatments.

Table 1 shows that the adsorption of C_2H_4 at 298 K, as well as the products of its pyrolysis, enhance the I_{rel} of UDP. It is known [8, 9] that the surface of ferromagnetics is partially or completely demagnetized. Therefore, an increase in the magnetization of nickel observed upon the adsorption of ethylene and the products of its pyrolysis can be associated with the additional orientation of surface nickel atoms spins due to the participation of adsorbate electrons in exchange interactions that determine magnetization. The one-mode dependence of magnetization on the coverages with ethylene and CH_x species indicates the same mechanism of an increase in magnetization. Magnetization growth upon chemisorption was observed in the case of hydrogen adsorption on island nickel films [10].

Oxygen adsorption. A choice of the temperatures for the O_2 adsorption is determined by the fact that it was found earlier for the island nickel films [11] that adsorbed oxygen is dissolved with increasing temperature (O-s $\longrightarrow$ O-v transition symbols s and v denote the surface and bulk oxygen, respectively), and the surface phase of nickel oxide with a Néel temperature of ~553 K (T_N(NiO) = 520 K [12]) is formed. The Curie temperature, T_C, of nickel films was 613 K, which corresponds to the T_C of bulk nickel. The data on an increase in the fraction of oxygen dissolved in the subsurface layer (O-v) in the presence of pyrocarbon was obtained earlier and

Table 2. Effect O_2 and H_2 on the relative magnetization I_{rel} of Ni UDP

Treatment		Nonmodified nickel UDP		Modified nickel UDP ($\theta_m = 0.1$)	
		I_{rel}	I_{rel}/I_{rel}^{0*}	I_{rel}	I_{rel}/I_{rel}^{0**}
Before adsorption at 298 K		64	1.00	74	1.00
Adsorption of O_2 at T, K	298	63	0.98	54	0.73
	523	83	1.30	56	0.76
	623	64	1.00	72	0.97
Evacuation of O_2 at 623 K after adsorption		56	0.90	68	0.92
Recovery with H_2 at 623 K	before recovery	58	1.00	68	1.00
	after recovery	50	0.86	116	1.70

* Before treatment in O_2 ($I_{rel}^0 = 64$) and H_2 ($I_{rel}^0 = 58$).

** Before treatment in O_2 ($I_{rel}^0 = 74$) and in H_2 ($I_{rel}^0 = 68$).

explained by an increase in the electron density in the vicinity of the CH_x species [13]. This increase causes an increase in the local work function that retards the formation of the negatively charged species O-s of atomic oxygen on the surface and favors the formation of the O-v species.

Table 2 shows that, upon the contact of an nonmodified sample with oxygen at room temperature, the magnetization of UDP did not change. When the temperature of adsorption was 523 K, the magnetization increased by 30%, and it decreased to I_{rel}^0 when the temperature of adsorption was 623 K. An increase in the magnetization of initial nonmodified UDP upon treatment with O_2 at 523 K (as in the case of the ethylene chemisorption) can be explained by a change in the state of the surface due to polarized oxygen atoms. A decrease in the magnetization of initial UDP upon high-temperature adsorption (T = 623 K), as well as after O_2 evacuation at this temperature, is due to the O-v $\longrightarrow$ O-s process and the removal of weakly bound oxygen.

O_2 adsorption (chemisorption) affects magnetization in a different manner in the case of a modified sample. At 298 and 523 K, the I_{rel} values decrease as compared to I_{rel}^0; at T = 623 K, I_{rel} coincides with that obtained before UDP contacted oxygen, as in the case of the nonmodified surface. A decrease in magnetization upon O_2 adsorption (chemisorption) is caused by an increase in the fraction of oxygen dissolved in the subsurface layer. The state of chemisorbed oxygen in the O-s–O-v–Ni complex with an increased content of O-v species on the modified sample differs from that on "clean" UDP.

The recovery of UDP with adsorbed oxygen by reduction in hydrogen is most efficient in the case of a nonmodified sample: the magnetization increases by a factor of 1.7, whereas the effect of recovery is absent for the initial UDP. A qualitatively similar result was obtained for island nickel films during the study of the $O_{ads} + H_2$ reaction. Thus, the introduction of pyrocarbon prepared from C_2H_4 resulted in an increase in the reaction rate in the case of paramagnetic nickel by ~20% and a decrease in the activation energy from 75 to 60 kJ/mol [14].

The kinetics of the $O_{ads} + CO \longrightarrow CO_2$ reaction. The initial reaction rates were determined from the linear kinetic curves for initial UDP and that dosed by pyrocarbon with 0.1, 0.2, and 1.6 of ML coverages. The extent of a decrease in O_{ads} calculated from the CO consumption was equal to 15–29%. The temperature dependences of the initial reaction rate are shown in the figure. The following orders with respect to CO (n) and O_{ads} (m) at 473 K were obtained:

	Pyrocarbon coverage, θ_m			
	0	0.1	0.2	1.6
n	1.5	0.75	0.75	1.3
m	1	0	0	0

The introduction of pyrocarbon changes the reaction orders and the temperature dependence of the reaction rate. The reaction rates on the "clean" surface of UDP pass through a maximum near 473 K and decrease with increasing temperature after the introduction of 0.1 and 0.2 ML of pyrocarbon. When the pyrocarbon content is higher than a monolayer, the reaction rates decrease and the temperature coefficient of the dependence $W = f(T)$ becomes positive. The apparent activation energy on the initial UDP is equal to 16 kJ/mol, which agrees with the data of [15]. The activation energy is 32 ± 3 kJ/mol for the modified surface (1.6 ML). An increase in the activation energy and a decrease in the preexponential factor point to UDP deactivation at a high pyrocarbon coverage; the reaction occurs on a

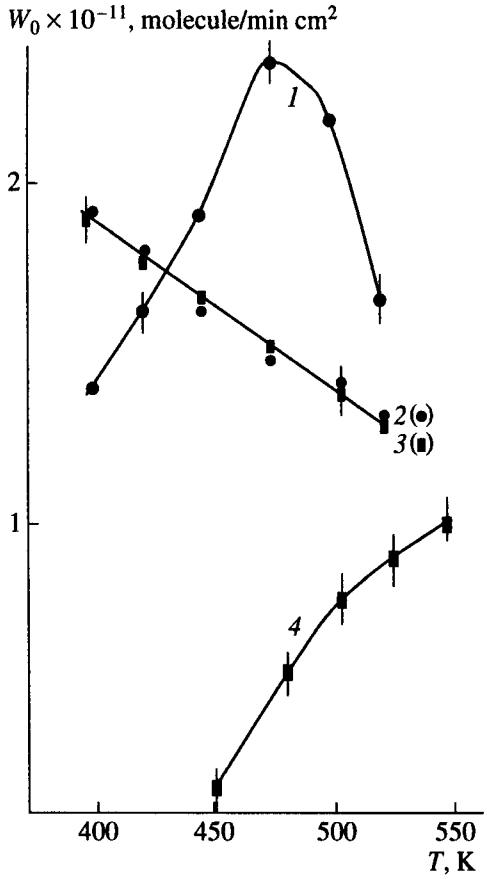

Temperature dependences of the initial rate of the CO + O_{ads} reaction over nickel UDP before (*1*) and after dosing the surface by pyrocarbon with coverages (*2*) 0.1, (*3*) 0.2, and (*4*) 1.6 ML.

small number of catalytically active sites that differ from those on the initial surface.

The dependences $W = f(T)$ with a maximum was also observed in the reactions CO + O_2 and CO + O_{ads} over other VIII-group metals (Pt catalysts [16] and Pd films [17]). A decrease in the oxidation rate of CO at 400–470 K associates with a decrease in the CO surface concentration (a decrease in the CO sticking coefficient) [16, 17]. At $T > 473$ K, the dissociation of adsorbed CO molecules starts on the nickel surface [18]. The data obtained for the island nickel films also provide evidence for CO dissociative adsorption accompanied by the dissolution of O_{ads} in the subsurface bulk of nickel particles [19]. According to [20], oxygen penetrates into the bulk most efficiently near the defects sites.

After dosing with pyrocarbon, the reaction order with respect to O_{ads} (m) decreased from unity to zero. The m value did not depend on θ_m. The same result was obtained for nickel films dosed by pyrocarbon in the $H_2 + O_{ads}$ reaction [11, 14]. The reaction order with respect to CO (n) decreased from 1.5 to 0.75 at small amounts of a modifying agent, and it was equal to 1.3 at $\theta_m = 1.6$. That is, the reaction order with respect to CO depended on the amount of pyrocarbon. Thus, we suggest that the reaction schemes for "clean" and modified surfaces of UDP are different.

Various reaction schemes were qualitatively examined to rationalize changes in experimental reaction orders. The following simple schemes proved to be preferable (the rate-determining steps are shown in boldface):

for the nonmodified surface

$$\begin{aligned} &1.\ CO_g + O\text{-}s \longleftrightarrow COO\text{-}s\ (K_1), \\ &\mathbf{2.\ CO_g + COO\text{-}s \longrightarrow CO_2\uparrow + CO\text{-}s}\ (k_2); \end{aligned} \quad \text{(I)}$$

for the modified surface at $\theta_m \leq 0.2$

$$\begin{aligned} &1.\ CO_g + s \longleftrightarrow CO\text{-}s\ (K_1), \\ &2.\ O\text{-}s + v \longleftrightarrow O\text{-}v + s\ (K_2 = k_2/k_{-2}), \\ &\mathbf{3.\ CO\text{-}s + O\text{-}s \longrightarrow CO_2\uparrow + 2s}\ (k_3). \end{aligned} \quad \text{(II)}$$

The rate-determining step in scheme (I) represents the interaction between CO molecules in the gas phase and the surface complex including two adjacent species, O_{ads} and CO_{ads}. The reaction rate is

$$W^0 = k_2 P_{CO}[COO\text{-}s] \quad (1)$$

or

$$W^0 = k_2 P_{CO} \frac{K_1 P_{CO}}{1 + K_1 P_{CO}} = k_2 P_{CO}^2 \frac{K_1}{1 + K_1 P_{CO}}. \quad (1')$$

Hence, the reaction order with respect to CO is higher than 1, in agreement with the experiment. The schemes for the formation of the surface carbonate structures considered by us contradict the experimental data.

As mentioned above, the modifying agent favors oxygen exchange between the surface and the bulk (dissolution), which was taken into account in scheme (II).

The reaction rate over the modified sample is

$$W_m^0 = k_3[O\text{-}s][CO\text{-}s] \quad (2)$$

or

$$W_m^0 = k_3[O\text{-}s] \frac{K_1 P_{CO}}{1 + K_1 P_{CO}}. \quad (2')$$

Equation (2') corresponds to the experimental data (the order with respect to CO can be lower than 1).

Taking into account step 2 (scheme (II)), we obtain the following expression for the surface concentration of oxygen:

$$[O\text{-}s] = \frac{k_{-2}[O\text{-}v]}{k_2(1 - [O\text{-}v]) + k_{-2}[O\text{-}v]}. \quad (3)$$

The oxygen concentration on the surface is controlled by the O-s + v ⟷ O-v + s step, which maintains the constancy of [O-s]. When the amount of adsorbed oxygen increases, a fraction of oxygen is dis-

tributed over the subsurface bulk and the amount of surface species virtually does not change. Therefore, the reaction rates are independent of the initial coverage by oxygen (the order with respect to O_{ads} is zero).

After dosing UDP by pyrocarbon at $\theta_m = 1.6$ ML, all adsorption sites are blocked by the modifying agent, and the reaction can occur via a Eley–Rideal mechanism: CO reacts with the surface oxygen, which is in equilibrium with the dissolved species O-v.

According to scheme (II), a decrease in the reaction rate upon dosing (0.1 and 0.2 ML) and a temperature increase from $T > 427$ K can be explained not only by a decrease in the surface concentrations of CO_{ads} and O_{ads} [14, 15] but also by an increase in the binding energy with the surface for CO_{ads} and O_{ads} reacting in step 3 (scheme (II)). As a result, $E_a = E^0 - E_O - E_{CO}$, where E_a and E^0 are the experimental and true activation energies, respectively. An increase in the binding energy (adsorption heat) of reactants mentioned above is due to an increase in the electron density on metal in the presence of positively charged species of the modifying agent at low surface concentrations [13]. Notably, in the low-temperature region ($T < 427$ K), small surface additives of pyrocarbon promote the activity of nickel UDP, and this requires a further study.

At a high concentration of the modifying agent ($\theta >$ 1 ML), the reaction occurs on other catalytically inactive sites, which are characterized by the low values of E_O and E_{CO}; therefore, $E_a > 0$.

CONCLUSION

Thus, the above results give evidence on the effect of dosing the surface of nickel UDP by the products of ethylene pyrolysis on the magnetization, state of chemisorbed oxygen, and its ability to interact with hydrogen and CO. The inhibiting effect of pyrocarbon on the $CO + O_{ads}$ reaction was established, which associates with an increase in the solubility of O_{ads} in the subsurface of the metal, the deactivation of the active sites, and a change in the reaction pathway. The action of small (less than a monolayer) and great (more than a monolayer) amounts of the modifying agent is different: in the first case, this action consists in that the binding energies of O and CO with the surface increase along with site blocking. In the second case, this action results in site blocking and the participation of other, catalytically inactive sites in the reaction.

REFERENCES

1. Node, M., Sinoda, S., and Saito, Ya., *Nippon Kagaku Kaishi*, 1984, no. 6, p. 1017.
2. Khayasi, T. and Nakayama, T., *Nippon Kagaku Kaishi*, 1984, no. 6, p. 1050.
3. Salova, O.S., Mikhalenko, N.N., Serov, Yu.M., and Gryaznov, V.M., *Zh. Fiz. Khim.*, 1991, vol. 65, no. 1, pp. 81–2543.
4. Khosiyama, I., Song, Yu.I., and Kim, T.S., *Nippon Kikei Gakkai Rombunsu, Ser. I*, 1983, vol. 49, no. 447, p. 2465.
5. Khayasi, T., *Sekubai*, 1985, vol. 27, no. 7, p. 437.
6. Coulter Model N4SD Sub-Micron Particles Analyser with Size Distribution Processor Analysis (Product Reference Manual), Techn. Commun. Coulter Electronics, 423559/Aug., 1985, p. 21.
7. Hudson, D., *Statistics: Lectures on Elementary Statistics and Probability*, Geneva, 1964.
8. Libermann, L., Clinton, J., and Edwards, D.M., *Phys. Rev. Lett.*, 1970, vol. 25, no. 4, p. 232.
9. Wang, D.S. and Freemann, A.J., *Phys. Rev. B: Condens. Matter*, 1981, vol. 24, no. 2, p. 1126.
10. Mikhalenko, I.I. and Yagodovskii, V.D., *Kinet. Katal.*, 1982, vol. 23, no. 3, p. 707.
11. Katre, A.M., *Cand. Sci. (Chem.) Dissertation*, Moscow: University of Peoples' Friendship, 1988.
12. Nagaev, E.L., *Physics of Magnetic Semiconductors*, Moscow: Mir, 1983, p. 87.
13. Yagodovskii, V.D. and Rei, S.K., *Zh. Fiz. Khim.*, 1982, vol. 56, no. 9, p. 2361.
14. Mikhalenko, I.I., Sarychev, V.I., Katre, A.M., and Yagodovskii, V.D., *Mater. IV Vsesoyuznoi konferentsii po kinetike geterogenno-kataliticheskikh reaktsii* (Proc. IV All-Union Conf. on Kinetics of Heterogeneous Catalytic Reactions), Moscow: Nauka, 1988, p. 87.
15. Labohm, F., Gijzeman, O.L.J., and Geus, J.W., *Surf. Sci.*, 1983, vol. 135, nos. 1–3, p. 409.
16. Boreskov, G.K., *Geterogennyi kataliz* (Heterogeneous Catalysis), Moscow: Nauka, 1988, p. 189.
17. Sarychev, V.I., *Cand. Sci. (Chem.) Dissertation*, Moscow: University of Peoples' Friendship, 1988.
18. Labohm, F., Charles, W.R., Gijzeman, O.I.J., and Geus, J.W., *J. Chem. Soc., Faraday Trans. 1.*, 1982, vol. 78, no. 8, p. 2435.
19. Katre, A.M., Mikhalenko, I.I., and Yagodovskii, V.D., *Zh. Fiz. Khim.*, 1988, vol. 62, no. 3, p. 703.
20. Matsueda, H. and Averbach, B.L., *Trans. Jpn. Inct. Metals*, 1983, vol. 24, no. 8, p. 574.